Article

Harnessing the Mechanism of Glutathione Reductase for Synthesis of Active Site Bound Metallic Nanoparticles and Electrical Connection to Electrodes

Daniel Scott, Michael Toney, and Martin Muzikr

J. Am. Chem. Soc., **2008**, 130 (3), 865-874 • DOI: 10.1021/ja074660g

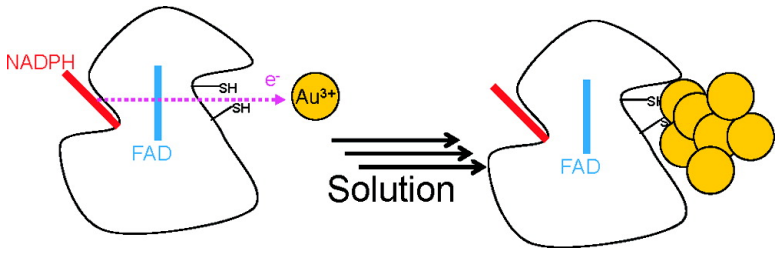

More About This Article

Additional resources and features associated with this article are available within the HTML version:

- Supporting Information
- Links to the 3 articles that cite this article, as of the time of this article download
- Access to high resolution figures
- Links to articles and content related to this article
- Copyright permission to reproduce figures and/or text from this article

View the Full Text HTML

J|A|C|S
ARTICLES
Published on Web 01/01/2008

Harnessing the Mechanism of Glutathione Reductase for Synthesis of Active Site Bound Metallic Nanoparticles and Electrical Connection to Electrodes

Daniel Scott, Michael Toney,* and Martin Muzikár*

Department of Chemistry, University of California, Davis, California 95616

Received June 25, 2007; E-mail: mdtoney@ucdavis.edu; mmuzikar@ucdavis.edu

Abstract: It is demonstrated herein that the FAD-dependent enzyme glutathione reductase (GR) catalyzes the NADPH-dependent reduction of $AuCl_4^-$, forming gold nanoparticles at the active site that are tightly bound through the catalytic cysteines. The nanoparticles can be removed from the GR active site with thiol reagents such as 2-mercaptoethanol. The deep enzyme active site cavity stabilizes very small metallic clusters and prevents them from aggregating in the absence of capping ligands. The behavior of the GR−nanoparticle complexes in solution, and their electrochemical properties when immobilized on graphite paper electrodes are presented. It is shown that the borohydride ion, a known reducing agent for GR, is catalytically oxidized by larger GR−nanoparticle (≥150 gold atoms) complexes generating catalytic currents, whereas NADPH (the natural reducing agent for GR) is not. It is proposed that the surface of the Toray graphite paper electrode employed here interferes with NADPH binding to the GR−nanoparticle complex. The catalytic currents with borohydride begin at the potential of GR-bound FAD, showing that there is essentially zero resistance to electron transfer (i.e., zero overpotential) from GR-bound FAD through the gold nanoparticle to the electrode.

Introduction

Nanotechnology and biotechnology are two fields of increasing importance that are merging. The former is focused on the synthesis, properties, and applications of nanometer-scale structures, whereas the latter exploits the extraordinary properties of biomolecules to solve significant medical, chemical, and engineering problems. The number of applications from the intersection of these two fields continues to increase.[1,2] Any one of these applications depends on the ability to control the chemistry of metal reduction on the nanometer scale. One popular conception of bionanoassemblers is that of using the specificity of biological macromolecules to control nanofabrication.

Biomimetic approaches have found success in utilizing proteins and specific peptide sequences to form well-defined nanostructures. Examples include the use of protein cage[3] and virus protein structures,[4] proteins containing peptide sequences that bind to specific metal faces,[5] or arrays of antibodies with metal-reducing sugars[6] as templates for nanoparticle synthesis.

In some cases, the product of an enzyme catalyzed reaction reduces metal ions to form nanoparticles[7] or proteins and enzymes were combined with nanoparticles to design biosensors.[8] However, to the best of our knowledge, there is no published work in which the natural catalytic activity of an enzyme is harnessed to reduce metals and form nanoparticles. Such an enzymatic reaction would provide a method for nanoparticle formation under conditions that: (1) have a defined number of initiation/reduction sites, (2) enable the formation of very small nanoparticles with precisely controlled size, and (3) expand the current paradigm for biomimetic nanoparticle syntheses.

There is strong evidence in the literature that biological systems commonly reduce free metal ions.[9−11] Additionally, it has been demonstrated that bacteria, fungi, and plants can facilitate gold nanoparticle (AuNP) synthesis from gold salts,[12−16] although the exact nature of AuNP synthesis in these systems has not been established.

It was reasoned that any redox-active enzyme with an active site poised at a potential capable of reducing metal ions might form metallic nanoparticles if metal reduction does not prevent

(1) West, J. L.; Halas, N. J. *Annu. Rev. Biomed. Eng.* **2003**, *5*, 285−292.
(2) Xiao, Y.; Patolsky, F.; Katz, E.; Hainfeld, J. F.; Willner, I. *Science* **2003**, *299* (5614), 1877−1881.
(3) Meldrum, F. C.; Heywood, B. R.; Mann, S. *Science* **1992**, *257*, 522.
(4) Moa, C.; Solis, D. J.; Reiss, B.; Kottmann, S.; Sweeney, R.; Hayhurst, A.; Georgiou, G.; Iverson, B.; Belcher, A. M. *Science* **2004**, *303*, 213−217.
(5) McMillan, R. A.; Paavola, C. D.; Howard, J.; Chan, S. L.; Zaluzec, N. J.; Trent, J. D. *Nat. Mater.* **2002**, *1*, 247.
(6) Jerry, Y.; Michael, M.; Kriebel, J. K.; Garstecki, P.; Whitesides, G. M. *Angew. Chem. Int. Ed.* **2004**, *43* (12), 1555−1558.
(7) Xiao, Y.; Pavlov, V.; Levine, S.; Niazov, T.; Markovitch, G.; Willner, I. *Angew. Chem. Int. Ed.* **2004**, *43* (34), 4519−4522.
(8) Daniel, M. C.; Astruc, D. *Chem. Rev.* **2004**, *104* (1), 293−346.
(9) Barkay, T.; Miller, S. M.; Summers, A. O. *FEMS Microbiol. Rev.* **2003**, *27* (2−3), 355−384.
(10) Lloyd, J. R.; Lovley, D. R.; Macaskie, L. E. *Adv. Appl. Microbiol.* **2003**, *53*, 85−128.
(11) Schuler, D. *J. Mol. Microbiol. Biotechnol.* **1999**, *1* (1), 79−86.
(12) Kashefi, K.; Tor, J. M.; Nevin, K. P.; Lovley, D. R. *Appl. Environ. Microbiol.* **2001**, *67* (7), 3275−3279.
(13) Lovley, D. R. *Annu. Rev. Microbiol.* **1993**, *47*, 263−290.
(14) Nair, B.; Pradeep, T. *Cryst. Growth Des.* **2002**, *2* (4), 293−298.
(15) Shankar, S. S.; Ahmad, A.; Pasricha, R.; Sastry, M. *J. Mater. Chem.* **2003**, *13* (7), 1822−1826.
(16) Mukherjee, P.; Senapati, S.; Mandal, D.; Ahmad, A.; Khan, M. I.; Kumar, R.; Sastry, M. *ChemBioChem* **2002**, *3* (5), 461−463.

subsequent regeneration of the reduced enzyme form. With a large enough active site cleft, such an enzyme would provide stabilizing ligands (i.e., amino acid side chains) to the nanoparticle as it grows.

Glutathione reductase (GR) is a flavoenzyme of known structure[17] that catalyzes the NADPH-dependent reduction of oxidized glutathione via a disulfide exchange reaction involving two active site cysteine residues.[18] It is a dimer in solution held together by noncovalent interactions. GR accepts electrons from reduced NAD(P)H into noncovalently bound FAD to give the $FADH_2$ (reduced) enzyme form. The electrons from $FADH_2$ are then transferred to an internal disulfide bond formed between Cys42 and Cys47 in the active site. The reduced cysteines then catalyze reduction of oxidized glutathione via a disulfide exchange reaction. Importantly, the NADPH binding site and the Cys42-Cys47 disulfide (glutathione binding site) are on opposite faces of the FAD cofactor and the enzyme structure. Thus, in principle, the glutathione binding site could be occupied by metals and the FAD could still be reduced by NADPH.

In this paper, the ability of *E. coli* GR to reduce Au^{3+} through its catalytic cysteines is demonstrated. This is very similar to the cognate chemistry catalyzed by the homologous enzyme mercuric ion reductase, which plays a central role in bacterial resistance to mercurials.[9,19] We show that reduction of Au^{3+} occurs via NADPH-dependent, flavin-mediated electron transfer and generates nanoparticles that are stabilized by the GR active site. The properties of the resulting GR−nanoparticle complexes are explored in detail.

Experimental Section

Materials. $KHPO_4$ and triethanolamine (TEA) were purchased from EM Science. Preformed, 2-nm gold nanoparticles (1.5×10^{14} particles/mL) were purchased from Ted Pella, Inc. Oxidized glutathione (GSSG), reduced nicotinamide adenine dinucleotide phosphate (NADPH), $HAuCl_4$, cyanogen bromide-activated agarose for solid-phase nanoparticle synthesis, sodium borohydride and all other chemicals were purchased from Sigma-Aldrich. Toray graphite paper 60 was a gift from Ballard Fuel Cells. All solutions were prepared with Millipore ultrapure water system of resistivity 18.0 MΩ cm.

Overexpression and Purification of GR. GR overexpression and purification was performed according to a published procedure with slight modifications.[20] The gene for *E. coli* glutathione reductase (GR) was a gift from Professors Charles Williams and Scott B. Mulrooney at Michigan State University. It was subcloned into plasmid pProExb-Hta and overexpressed in *E. coli* BL21 DE3 gold. The harvested cells were resuspended in 100 mM potassium phosphate buffer pH 7.6, sonicated at 4 °C for 30 min, and centrifuged at 20 000 × *g* for 40 min. GR was purified from the supernatant using Ni-NTA Superflow resin (Qiagen) via the 6×His tag added to the GR gene in the pProExb-Hta-GR construct. The desired enzyme was eluted with 300 mM imidazole, dialyzed into 100 mM potassium phosphate buffer pH 7.6, and stored frozen at −70 °C.

Synthesis of Enzyme−AuNP. Synthesis of GR−AuNP was achieved by incubation of enzyme with NADPH and $AuCl_4^-$ in 100 mM phosphate buffer, pH 7.6. GR−AuNP with more than 50 Au atoms was prepared in multiple steps to keep NADPH and $AuCl_4^-$ concentrations below 5 mM, which minimizes nonenzymatic nanoparticle formation. For electrochemical experiments, samples in buffer were incubated on a round piece of Toray graphite paper. Incubation times varied for different experiments. Samples were covered to ensure minimal evaporation of solution. After the desired incubation time, the electrodes were rinsed thoroughly in 100 mM phosphate buffer pH 7.6. Control experiments for these electrodes followed the same procedure with slight modifications. For control reactions, either NADPH or $AuCl_4^-$ was withheld from the incubation.

UV−vis Spectrophotometry. The absorption spectra of GR-bound FAD were monitored using a Kontron 9300 UV−vis spectrophotometer. The spectrum of the oxidized form of the enzyme was taken from a solution of 110 μm GR in 100 phosphate buffer, pH 7.6, while the spectrum of the reduced form was obtained from incubation of 110 μm GR with 120 μm NADPH in the same buffer. GR catalyzed reduction of $AuCl_4^-$ in the presence of NADPH was also studied. The decrease in NADPH absorbance at 340 nm was used to determine the rate of GR catalyzed gold reduction.

Matrix-Assisted Laser Desorption/Ionization-Time Of Flight (MALDI-TOF). Formation of GR−AuNP complexes was studied by MALDI-TOF on a Perceptive Biosystems Voyager-DE and ABI 4700 at the Molecular Structure Facility at University of California−Davis. Samples were prepared by incubating GR, NADPH, and $AuCl_4^-$ together in buffered solution for 10 min at room temperature. After incubation, enzyme was passed over a Sephadex G25 spin column, mixed in a 1:1 ratio with a matrix solution of 60% acetonitrile saturated with sinapinic acid, and a 2-μL portion of sample was allowed to dry on the MALDI target.

Atomic Absorption Spectroscopy. Atomic absorption (AA) spectroscopy was used to determine the amount of reduced gold that bound to GR after incubation with $AuCl_4^-$ and NADPH. GR was incubated with different concentrations of NADPH and $AuCl_4^-$ aliquots in phosphate buffer, pH 7.6. In control reactions, NADPH was replaced with buffer. The excess NADPH and $AuCl_4^-$ were removed with Sephadex G25 spin columns pre-equilibrated in phosphate buffer. A standard curve was measured with freshly made samples of $AuCl_4^-$ in 10 mM HCl.

SDS-Polyacrylamide Gel Electrophoresis (SDS-PAGE). SDS-PAGE was used to study multimeric structures of enzyme after reduction of $AuCl_4^-$. Samples of GR−AuNP prepared by mixing GR, NADPH, and $AuCl_4^-$ aliquots in phosphate buffer, pH 7.6, which were incubated with and without different concentrations of 2-aminoethanethiol and run on 10% polyacrylamide using a loading buffer without 2-mercaptoethanol. Gels were run at 120 V for 70 min and stained with coomassie blue.

Transmission Electron Microscopy (TEM). A Philips 120 BioTwin electron microscope at 80KV equipped with a Gatan/MegaScan, model 794/20 digital camera was used to collect transmission electron microscope (TEM) images.

For TEM images, 44 μM GR, 10 mM NADPH and 3.4 mM $AuCl_4^-$ in 100 mM phosphate buffer, pH 7.6 were mixed to form GR−Au_{280}. The 280-atom gold nanoparticle corresponds to a sphere of about 2.1 nm. GR−Au_{280} was diluted 5-fold in water for TEM experiments, and 10 μL of sample were placed on a 400 mesh copper grid and allowed to evaporate.

Electrochemical Measurements. Electrochemical experiments were performed using a three-electrode system in a Pyrex glass electrochemical cell with a Teflon cap. The cell was enclosed in a Faraday cage, which was connected to a common ground. Experiments were carried out at 25 °C. The electrolyte solution of 100 mM phosphate buffer, pH 7.6 was purged for 30 min with argon before electrochemical experiments and kept under an argon atmosphere during the experiments. The Ag/ AgCl (3M KCl) electrode served as a reference and a platinum wire of about 1-mm diameter as the counter electrode. Working electrodes were made from Toray graphite paper discs that were 4 mm in diameter. A gold wire was twisted into a clip at its end, and the TGPE discs were held in place by insertion into this clip. Enzyme was immobilized on TGPEs by incubating the electrode in a

(17) Mittl, P. R. E.; Schulz, G. E. *Protein Sci.* **1994**, *3* (5), 799−809.
(18) Rietveld, P.; Arscott, L. D.; Berry, A.; Scrutton, N. S.; Deonarain, M. P.; Perham, R. N.; Williams, C. H. *Biochemistry* **1994**, *33* (46), 13888−13895.
(19) Engst, S.; Miller. S. M. *Biochemistry* **1999**, *38*, 853−854.
(20) Scrutton, N. S.; Berry, A.; Perham, R. N. *Biochem. J.* **1987**, *245*, 875−880.

solution of GR or GR−AuNP (30 μL of 0.4−4 μM in 100 mM potassium phosphate buffer, pH 7.4) for 30 min at room temperature. The immobilization reactions were covered to prevent evaporation.

For modification of TGPE electrode with gold nanoparticles, 4-mm disc-shaped TGPEs were incubated in 500 μL of 2-nm preformed gold nanoparticles overnight. The electrode was washed in five changes of 100 mM potassium phosphate buffer pH 7.4.

Working electrodes for measurement of $NaBH_4$ oxidation catalysis were 4-mm diameter, disc-shaped Toray graphite paper mounted by carbon conductive tape to a 3-mm diameter glassy carbon electrode.

CV experiments were performed with an Autolab PG STAT12 potentiostat/ galvanostat (ECO Chemie, The Netherlands) using a General-Purpose Electrochemical System plug-in (version 4.9.5) software and electrochemical impedance spectroscopy (EIS) experiments with an Autolab PG STAT30 using frequency response analyzer software.

Determination of the real electrode area was performed by measuring the limiting current for reduction of the ferricyanide anion from voltammograms obtained under steady-state conditions. The real area of the 4-mm working TGPE was determined to be 35.7 cm^2, corresponding to a roughness factor of 72, estimated using the published diffusion coefficient of 0.4 mM ferricyanide ($D = 7.65 \times 10^{-6} \pm 0.001$ cm^2 s^{-1}) ion with 0.05 M KCl as the supporting electrolyte.[21]

Cyclic Voltammetry. Cyclic voltammograms were collected for GR, GR−Au_5, GR−Au_{50}, GR−Au_{150}, and GR−Au_{250} on TGPEs.[22,23] The effect of noncompensated cell resistance was minimized by the correction to iR drop. Background electrode currents, which vary with scan rate, were subtracted from cyclic voltammograms by fitting polynomial curves at the potentials preceding and following the faradaic process.

FAD Redox Potential of GR−Nanoparticle Complexes as a Function of pH. The redox potential of the enzyme-bound FAD in GR−AuNP complexes immobilized on TGPE was studied as a function of pH for comparison to the free enzyme in solution. Phosphate buffer was used throughout the entire pH range studied. The redox potentials of FAD were determined by cyclic voltammetry at 100 mV/s scan rate; the averages of the oxidation and reduction peaks were plotted as a function of pH. Two other experiments were performed in which TGPEs were soaked in the free FAD and GR that had been denatured in 7 M guanidine hydrochloride. In all of these experiments, the concentration of FAD was constant at about 1.8 μM. The results obtained herein are compared with GR redox potentials obtained by Veine et al.[24]

Results

Reduction of $AuCl_4^-$ by GR. We initially tested the ability of $AuCl_4^-$ to oxidize the FAD cofactor of GR, previously reduced by NADPH. The spectra presented in Figure 1a show differences between oxidized and reduced GR-bound FAD, the latter obtained by the addition of NADPH (120 μM; 240 μM e^- equivalents) to the oxidized enzyme (110 μM). The addition of $AuCl_4^-$ (85 μM; 255 μM e^- equivalents required for complete reduction) to the reduced enzyme converted the FAD spectrum back to that of the oxidized enzyme, demonstrating electron transfer from NADPH to $AuCl_4^-$ mediated by FAD. The reoxidation of the FAD by $AuCl_4^-$ happened within the mixing time (~5 s).

The steady-state kinetics of GR-catalyzed $AuCl_4^-$ reduction were also examined, and the results are presented in Figure 1b.

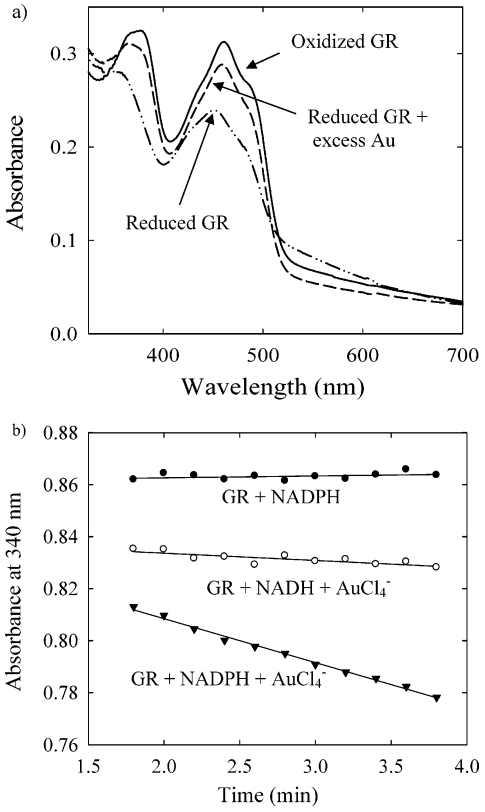

Figure 1. (a) Absorbance spectra of GR-bound FAD ([GR] = 110 μM, [NADPH] = 120 μM, [$AuCl_4^-$] = 85 μM) (b) Initial rates of nicotinamide cofactor oxidation. ([GR] = 14 μM, [NADPH] = [NADH] = 265 μM, [$AuCl_4^-$] = 72 μM). 0.8 absorbance units have been subtracted from the reported values due to the reference solution used.

In the absence of $AuCl_4^-$, the absorbance of NADPH (265 μM) at 340 nm in the presence of 14 μM GR is stable on the minute time scale. There is a low level of NADPH oxidation over a much longer time frame due to the presence of O_2 in the solution. The addition of $AuCl_4^-$ (72 μM) led to the rapid oxidation of NADPH. Control experiments both without enzyme and with varying concentrations of GR showed the oxidation to be catalyzed by GR. The reaction rate saturated with increasing concentrations of $AuCl_4^-$ and constant concentrations of GR and NADPH. Fitting the data to the Michaelis−Menten equation gave $K_m \approx 120$ μM and $k_{cat} \approx 1$ s^{-1}.

Although NADPH typically does not reduce metals, there is evidence in the literature for NADPH reducing $AuCl_4^-$.[25] However, it was found that by buffering the $AuCl_4^-$ solution with phosphate buffer (pH 7) and keeping the concentrations of $AuCl_4^-$ and NAD(P)H in the reactions below ~5 mM, no detectable reduction of $AuCl_4^-$ was observed within an hour.

Two other proteins were used as controls to show that $AuCl_4^-$ was reduced in the GR active site by FAD. When GR was replaced by bovine serum albumin (BSA), no detectable NADPH oxidation was observed. When an NADPH dependent secondary alcohol dehydrogenase was used in place of GR, oxidation of NADPH in the presence of $AuCl_4^-$ did not occur.

Replacement of NADPH in the reaction by NADH, whose structure differs by a single phosphate group and whose redox potential is essentially identical,[26] results in a decrease in reaction

(21) Adams, R. N. *Electrochemistry at Solid Electrodes*; Marcel Dekker Inc.: New York, 1969; p 219.
(22) Sucheta, A.; Cammack, R.; Weiner, J.; Armstrong, F. *Biochemistry* **1993**, *32*, 5455−5465.
(23) Leger, C.; Elliott, S.; Hoke, K.; Jeuken, L.; Jones, A.; Armstrong, F. *Biochemistry* **2003**, *42*, 8653−8662.
(24) Veine, D.; Arscott, D.; Williams, C. *Biochemistry* **1998**, *37*, 15575−15582.
(25) Kelly, M.; Brian, T.; Schaab, M.; Mills, G. *Abstracts of Papers, 224th ACS National Meeting*, 2002.
(26) Scrutton, N. S.; Berry, A.; Perham, R. N. *Nature* **1990**, *343*, 38−43.

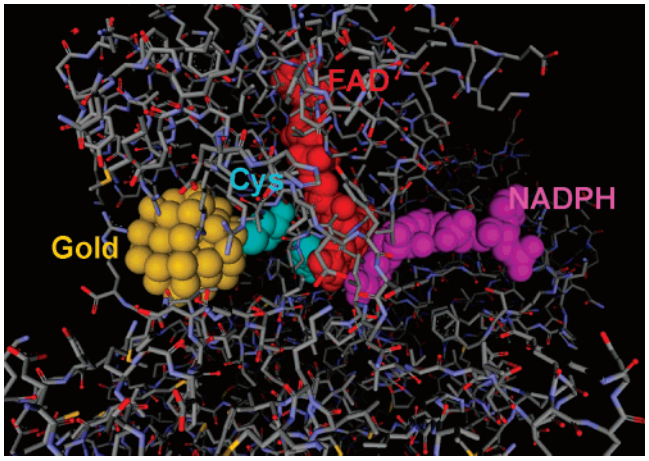

Figure 2. Space-filling model of the active site cleft of GR with a 55-atom gold nanoparticle. Cys47 is closest to FAD, whereas Cys42 is closest to the gold nanoparticle modeled into the structure.

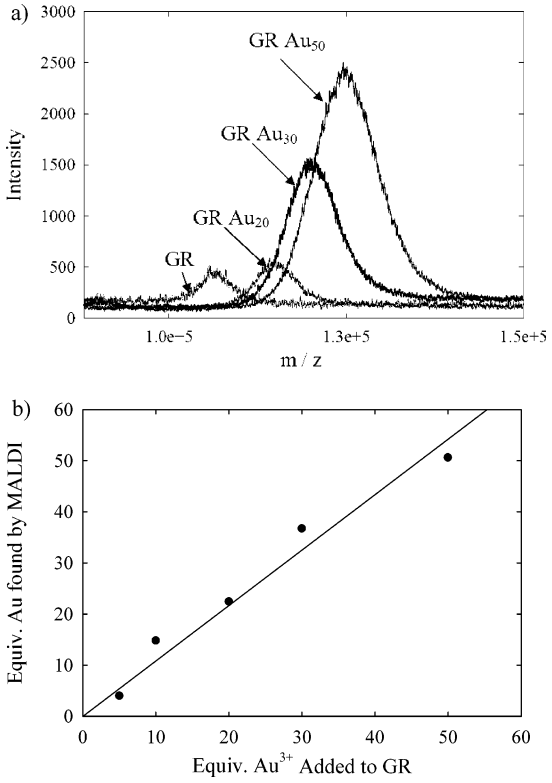

Figure 3. (a) MALDI-TOF mass spectra of GR reacted with an excess of NADPH and various stoichiometries of $AuCl_4^-$. (b) The linear correlation between the number of gold atoms added per enzyme active site and the number found by mass spectrometry.

rate (Figure 1b). This agrees with the well documented preference of *E. coli* GR for NADPH over NADH.[26]

Formation of GR−AuNP Clusters. Having established that GR catalyzes NADPH-dependent reduction of $AuCl_4^-$, it was hypothesized that the reduced gold is tightly bound to the enzyme via interactions with an active site cysteine (Cys42; Figure 2). Results from tests of this hypothesis follow.

GR (45 μM) was incubated for 30 min with 4.5 mM NADPH, various stoichiometries of $AuCl_4^-$, and analyzed by MALDI-TOF (Figure 3a). The spectrum of the enzyme without $AuCl_4^-$ shows two peaks, one corresponding to the singly charged dimer at m/z = 105 600 and another corresponding to the singly

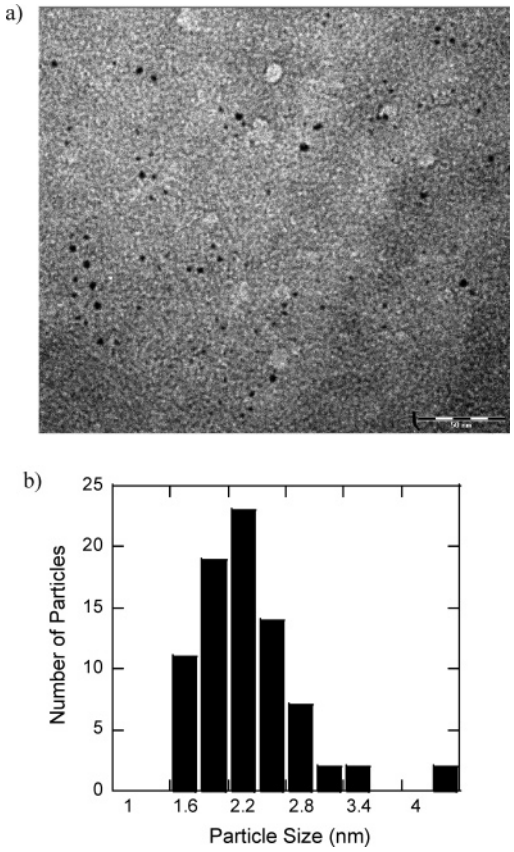

Figure 4. (a) TEM image of GR−Au_{280}. (b) A size histogram of 100 randomly chosen particles, with a mean diameter of 2.13 nm.

charged monomer at m/z = 52 800. The addition of 20 equiv of $AuCl_4^-$ per enzyme with excess NADPH produced a spectrum ("GR−Au_{20}" in Figure 3a) shifted by the mass of twenty gold atoms. Similar mass spectra were obtained for stoichiometries of 30 and 50. Figure 3b shows a linear correlation between the number of $AuCl_4^-$ molecules added per enzyme and the number of gold atoms found per enzyme by mass spectrometry. Remarkably, this linear correlation extends down to 5 atoms of gold per enzyme. Additionally, the mass spectral peak widths demonstrate a narrow distribution of gold cluster sizes among the enzymes.

The MALDI data were corroborated by atomic absorption experiments. As the stoichiometry of $AuCl_4^-$ to GR increased, a larger amount of GR-bound gold was detected by AA after passing the samples over size-exclusion spin columns to remove low molecular weight species (e.g., NADPH, $AuCl_4^-$) not bound to the enzyme. This increase was only observed in samples that contained NADPH.

The TEM image in Figure 4a confirms that AuNPs are formed by GR. The particle diameter histogram in Figure 4b agrees with the expected Au_{280} nanoparticle size. One hundred randomly chosen particles had a mean diameter of 2.13 nm, which matches with the predicted diameter of 2.1 nm.

The MALDI-TOF spectra show an increase in the dimeric form of GR as the size of the gold nanoparticle increases, even under the harsh conditions of the MALDI matrix (saturated sinapinic acid in 65% acetonitrile). SDS-PAGE experiments gave similar results (Figure 5). After the enzyme reduces ~6 atoms of gold, the band at the mass of the dimeric form of the enzyme increases (data not shown). This band continues to

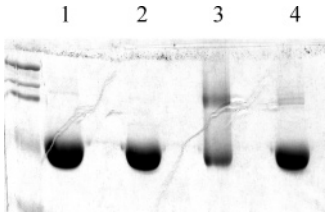

Figure 5. SDS-PAGE experiment: (1) GR; (2) GR in 50 mM 2-aminoethanethiol; (3) GR−Au_{50}; and (4) GR−Au_{50} in 50 mM 2-aminoethanethiol.

increase to ∼50% of the enzyme in its dimeric form after it has reduced ∼18 atoms of gold (see Supporting Information). As more gold is reduced by GR, the increase in the amount of the dimeric form continues. Upon the addition of a thiol reagent such as 2-aminoethanethiol or 2-mercaptoethanol, the enzyme, under denaturing conditions, returned to its predominantly monomeric form.

When the nanoparticles are <2.5 nm and GR is not denatured, the complexes do not show a plasmon resonance absorption band. If the enzyme is allowed to reduce more than ∼280 $AuCl_4^-$ per active site, then the solution turns red and TEM shows the formation of larger aggregates (10−50 nm). Nanoparticle aggregation, with the resultant appearance of a plasmon resonance absorption band, also occurs when the GR−AuNP complex (even with less than 280 atoms of gold) is left at room temperature overnight. These results are consistent with the sequestration of the nanoparticle from solvent (and other nanoparticles) by the deep active site cleft. Sterically, this prevents aggregation of the reduced gold until either the nanoparticle grows large enough to protrude out of the active site and collide with other protruding nanoparticles, or the protein structure is disrupted by denaturation.

Inhibition and Reactivation of GR and GR−AuNP. Here, GR activity assays were performed in 100 mM phosphate buffer, pH 7.6, 0.76 μM GR, 0.26 mM NADPH and 0.5 mM GSSG at room temperature. When $AuCl_4^-$ was incubated with GR in a 10:1 molar ratio in the presence of NADPH, GR was >90% inactivated toward GSSG reduction after 4 min. In the absence of NADPH, samples remained >90% active after 30 min.

When 2-nm preformed particles were incubated with 54 μM GR in a 1.2:1 ratio in the presence of 0.5 mM NADPH, >99% of GR activity toward GSSG was lost within 45 s. In the absence of NADPH, >75% of the original activity remained after 20 min of incubation.

In another experiment, GR was alkylated at the distal active site cysteine. Here, 25 μM GR was incubated with 3 mM iodoacetamide and 2.8 mM NADPH in phosphate buffer, pH 7.6 for 3 h. Excess NADPH and iodoaceamide were removed by a Sephadex G-25 spin column. A control reaction without NADPH was included. Under these conditions, Cys42 was alkylated and GR was inactive toward either glutathione or gold reduction.[27]

Finally, when 9 μM GR was reacted with 15% H_2O_2 for 1 min in the presence of 0.24 mM NADPH, the active site cysteine was oxidized and GR was inactive toward both GSSG and $AuCl_4^-$ reduction. This activity loss did not occur when NADPH was replaced by $NADP^+$ in the reaction. FAD bound to the active site of the H_2O_2-oxidized GR still accepted electrons from NADPH, as determined from the absorption spectrum.

(27) Stryer, L. *Biochemistry*, 4th ed.; W. H. Freeman and Company: New York, 1999.

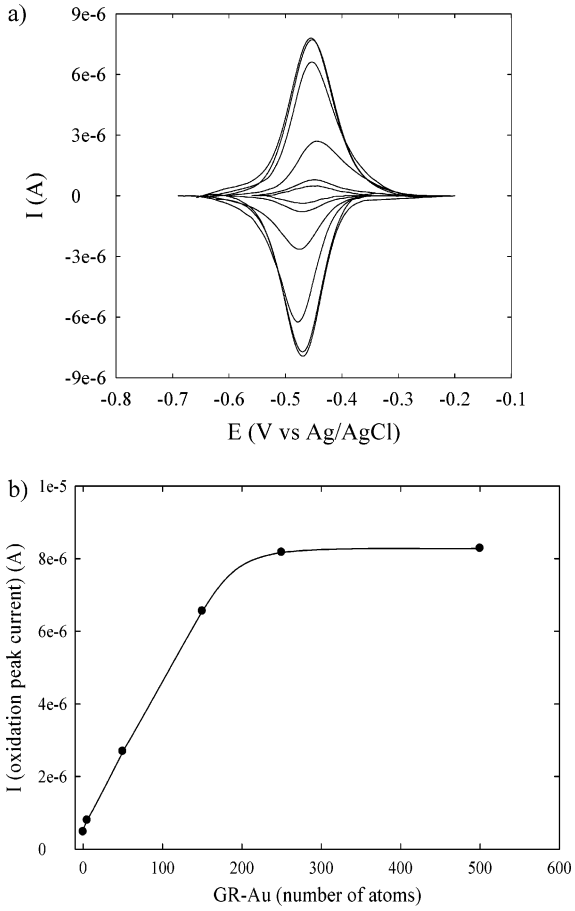

Figure 6. (a) Increase in FAD current as the function of nanoparticle size in the enzyme's active site. Cyclic voltammograms correspond to GR, GR−Au_5, GR−Au_{50}, GR−Au_{150}, GR−Au_{250}, and GR−Au_{500} (lowest to highest). (b) The increase of FAD oxidation current plotted vs the number of atoms in enzyme's active site. Conditions: 100 mM phosphate buffer, pH 7.6, 200 $mV.s^{-1}$ scan rate.

Oxidase Activity of the GR−Gold Nanoparticle Complex. It was shown that 10, 20, and 40 gold atoms attached to the enzyme increased the rate of NADPH consumption in air-equilibrated 100 mM phosphate buffer, pH 7.6, in the absence of Au^{3+} or glutathione. The 10, 20, and 40 gold atoms in the GR active site corresponded to 2.3-, 3.0-, and 4.7-fold increases in NADPH oxidation compared to GR alone (Figure 6 in Supporting Information). When the samples were bubbled with O_2 gas for 30 s, the NADPH oxidation rate doubled. When the same sample was purged with argon for 30 s, NADPH oxidation was not detectable. When the sample was re-exposed to O_2, the NADPH oxidation activity returned. This demonstrates that when the size of the nanoparticle in the GR−AuNP complex increases, a corresponding increase in the rate of oxygen reduction is observed. This is consistent with an increase in the area of the gold surface active in reducing oxygen as the nanoparticle size increases.

Solid-Phase Nanoparticle Synthesis. GR immobilized on cyanogen bromide-activated agarose resin from 50 mM potassium phosphate buffer, pH 7.6 retained its activity toward GSSG and $AuCl_4^-$. Suspension of the GR-modified resin in buffer containing $AuCl_4^-$ and NADPH produced resin-bound gold nanoparticles. The GR−Au_{200} resin-bound complex was prepared in four Au_{50} reaction steps. Each step was allowed to proceed for 10 min.

After completion of nanoparticle synthesis, the resin was first washed with 50 mM potassium phosphate buffer, which was followed by addition of 2-mercaptoethylamine to 15 mM and incubation for 2 h to release the nanoparticles. Gold nanoparticles were separated from the resin, and TEM was used to analyze the buffered 2-mercaptoethylamine solution before and after exposure to the resin. Only in the sample that was exposed to the resin, TEM confirmed the presence of individual gold nanoparticles of ~2 nm, which is in agreement with the expected ~200 atoms of gold per enzyme in this experiment.

Electrochemical Study of GR−AuNP Clusters. Cyclic voltammograms (CVs) of GR immobilized on Toray graphite paper electrodes (TGPEs) showed reversible electron transfer with sharp voltammetric signals at the potential characteristic for FAD bound to the GR.[24] When the TGPE was soaked in 100 mM phosphate, pH 7.4 containing 0.44 μM GR for 30 min, small oxidation and reduction peaks of ~0.47 μA at a scan rate of 100 mV s^{-1} were observed. When the immobilization time for GR was extended to 24 h, there was no significant increase in FAD current. The same current at the same potential was found in control experiments where the electrode was soaked in GR and NADPH without $AuCl_4^-$, and GR and $AuCl_4^-$ without NADPH. When GR was immobilized on TGPE preoxidized by incubation in nitric acid solution overnight at room temperature, an approximately 2-fold increase in FAD current peak was observed. This finding strongly suggests that the enzyme is immobilized on the TGPE by hydrophilic interactions.

After incubating a TGPE in a buffered solution of GR, $AuCl_4^-$, and NADPH (or in GR−AuNP solutions made from preformed nanoparticles) for 30 min, the oxidation and reduction currents at the potential of FAD significantly increased. For example, when a TGPE was incubated in mixtures of GR and $AuCl_4^-$ in molar ratios of 1:5, 1:50, 1:150, and 1:250, oxidation and reduction currents in CVs increased 2, 6, 15, and 18 fold, respectively (Figure 6). When the gold nanoparticle size exceeded 150 atoms, the current increase slowed and eventually remained constant with further increases in nanoparticle size. That the enzyme forms a stable layer on the electrode surface was demonstrated by a lack of change in the oxidation and reduction peak areas after 5 h for GR and GR−AuNP.

It is important to verify that the current increase is not produced by greater enzyme immobilization in the presence of gold nanoparticles during the fixed time of the TGPE soak. Electrochemical impedance spectroscopy (EIS) was used to compare the amount of GR and GR−AuNP immobilized on TGPE (see Supporting Information). The change in charge-transfer resistance of the $Fe(CN)_6^{3-/4-}$ redox probe was monitored after the binding of GR and GR−AuNP.[28] The charge-transfer resistance for GR−AuNP modified TGPEs was ~1.5 fold greater than that for GR-modified TGPEs, suggesting either a slightly greater rate of immobilization for the GR−AuNP or a slighter higher number of binding sites for the GR−AuNP complex, depending on the kinetics of the immobilization.

The EIS results were corroborated by direct assay of the amount of protein bound to the TGPE. GR, GR−Au_{50}, and GR−Au_{250} were immobilized on a TGPE for 30 min, then removed from it by boiling in 1% SDS for 30 min. The protein concentration in the SDS extracts was determined spectrophotometrically using the Bio-Rad DC protein assay. Enzyme immobilization for GR, GR−Au_{50} and GR−Au_{250} was identical within experimental error (~25%; see Supporting Information).

It was also determined from the FAD half-height peak width (55−70 mV for GR and GR−AuNP, independent of the gold nanoparticle size) at slow scan rates[29] that 2 electrons are involved in the redox process for GR and all GR−AuNP complexes. The theoretical half-height peak width for a two electron-transfer process at 298 K is 45 mV. The slightly higher peak width observed in our experiments is due to signal dispersion from different orientations/environments that the immobilized enzyme experiences on the TGPE electrode.[30]

Enzyme surface coverage was calculated from the decrease in the real surface area after 30 min enzyme immobilization. Taking into account that one enzyme molecule covers ~30 nm^2, the surface coverage was estimated to be 9.5×10^{-13} mol cm^{-2}. This corresponds to ~17% surface coverage by GR.

pH Dependence of FAD Redox Potential in GR−AuNP. GR−Au_{50}, FAD and denatured GR were immobilized on a TGPE by soaking in 100 mM phosphate buffer for 30 min. The redox potentials were measured by cyclic voltammetry (scan rate 100 mVs^{-1}) as a function of pH. As the pH of the buffer increased, the potential of the redox reaction shifted toward negative potentials. This is consistant with an FAD molecule.[31] As the pH increases, the reduced FAD decreases in stability and a negative shift of the FAD potential is seen. The data (Figure 7) agree well with the pH dependence of the GR redox potential for enzyme in solution.[24]

Catalytic Borohydride Oxidation. GR−Au_{200} was immobilized for 30 min on a TGPE that was mounted by conductive carbon tape to a glassy carbon electrode. The gold wire used for other voltammetric experiments was avoided to eliminate direct oxidation of borohydride at gold. Cyclic voltammograms were measured at scan rates of 100 mVs^{-1} and a $NaBH_4$ concentration of 2 mM (Figure 8). Control experiments with 2 nm premade gold nanoparticles immobilized on TGPE overnight in the absence of GR were also performed to test if the GR-bound nanoparticle might be catalytically active independent of the enzyme bound to it (Figure 9).

Discussion

GR Catalyzed $AuCl_4^-$ Reduction. Remarkably, GR catalyzes the NADPH-dependent reduction of $AuCl_4^-$ to form active site bound metallic nanoparticles whose size can be tightly controlled over a broad range. To the authors' knowledge, this is the first example of harnessing the cognate mechanism of a redox enzyme for the direct reduction of metal ions leading to formation of a nanoparticle that is tightly bound to the active site. In related work, others have shown that enzymes can catalyze independent reactions whose products reduce metals in the solution,[32] that enzymes can facilitate biocatalytic enlargement of preformed nanoparticles,[33] and that gold nanoparticles external to the active site can facilitate electron transfer

(28) Katz, E.; Willner, I. *Electroanalysis* **2003**, *15*, 913−947.
(29) Laviron, E. *J. Electroanal. Chem.* **1979**, *100*, 263−270.
(30) Armstrong, F. A.; Camba, R.; Heering, H. A.; Hirst, J.; Jeuken, L. J. C.; Jones, A. K.; Léger, C.; McEvoy, J. *Faraday Discuss.* **2000**, *116*, 191−203.
(31) Tinoco, I.; Sauer, K.; Wang, J. C. *Physical Chemistry, Principles and Applications in Biological Sciences*, 2nd Ed.; Prentice−Hall: New Jersey, 1985; p 145.
(32) Willner, I.; Baron, R.; Willner, B. *Adv. Mater.* **2006**, *18*, 1109−1120.
(33) Zayats, M.; Baron, R.; Popov, I.; Willner, I. *Nano Lett.* **2005**, *5*, 21−25.

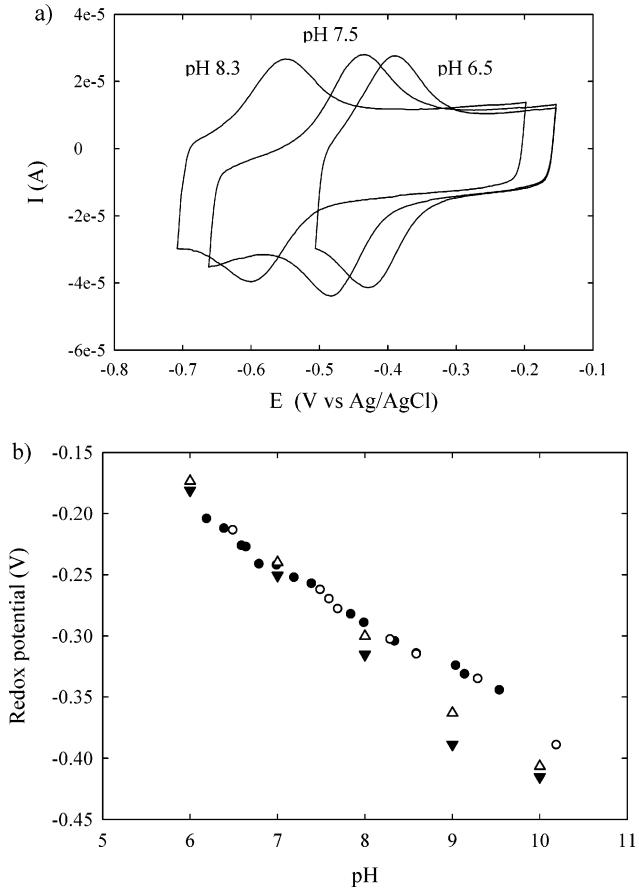

Figure 7. (a) Cyclic voltammograms of FAD at different pHs in 100 mM phosphate buffer; scan rate 100 mV•s^{-1}. (b) Plots of redox potentials vs pH: denatured GR (△), FAD (▼), GR−Au_{50} (○), and GR from literature (●).[24]

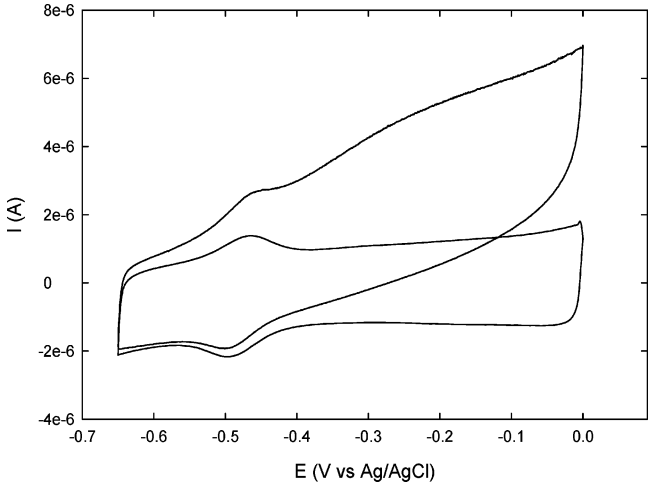

Figure 8. GR−Au_{200} immobilized for 30 min on a 4-mm disc TGPE mounted with carbon conductive tape to a 3 mm diameter glassy carbon electrode without $NaBH_4$ (lower CV) and with the addition of 2 mM $NaBH_4$ (upper CV). Conditions: 100 mM phosphate buffer, pH 7.4; scan rate 100 mV.s^{-1}.

between enzyme and electrode.[2] The novel nature of our findings demonstrate however that enzymes can indeed function as nanoassemblers, allowing defined nucleation and growth of redox active metallic nanoparticles that are protected by sequestration in the enzyme active site.

Absorption spectral changes verified that the path of the electrons is from NADPH to enzyme bound FAD to $AuCl_4^-$;

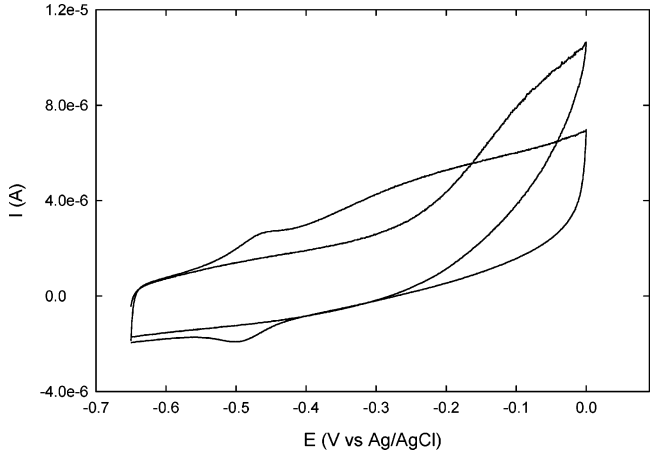

Figure 9. GR−Au_{200} immobilized on TGPE for 30 min and TGPE incubated overnight in 500 μL of 0.25 μM premade 2 nm gold nanoparticle solution. Conditions: 100 mM potassium phosphate pH 7.4, 2 mM $NaBH_4$; scan rate 100 mV.s^{-1}; The first CV cycle measured is reported here.

addition of NADPH to oxidized enzyme produces the known absorption spectrum of the reduced flavin and addition of $AuCl_4^-$ to this regenerates the oxidized form. The slightly blue-shifted spectrum of the reoxidized enzyme suggests that the $AuCl_4^-$ accepts electrons from FAD and concomitantly prevents disulfide bond formation between the active site cysteines.[34] Reoxidation of $FADH_2$ by $AuCl_4^-$ is rapid (over within the ∼5 s mixing time of the experiment), suggesting direct electron transfer from active site bound flavin to $AuCl_4^-$. Rapid flavin oxidation by $AuCl_4^-$ is also in agreement with the k_{cat} of ∼1 s^{-1} calculated from initial rates of NADPH oxidation. The structurally homologous FAD dependent enzyme mercuric ion reductase reduces Hg^{2+} to Hg^0 with a k_{cat} of ∼20 s^{-1}, not dissimilar to that observed here with GR and $AuCl_4^-$.[9]

Additional evidence that GR directly catalyzes the NADPH-dependent reduction of $AuCl_4^-$ was gathered. For example, the use of NADH instead of NADPH as the electron donor gives a lower rate of reduction; *E. coli* GR shows a strong preference for NADPH over NADH in glutathione reduction,[26] which is reflected in the noncognate $AuCl_4^-$reduction reaction as well. If the reaction were occurring somewhere other than the active site, then one would expect NADH and NADPH to be equally effective based on their redox potentials. Experiments with BSA and the NADPH-dependent secondary ADH provided results that also weigh against the possibility that the reaction is catalyzed by the surface of the protein or that the binding of NADPH to an active site is increasing the ability of NADPH to transfer electrons to $AuCl_4^-$ directly.

$AuCl_4^-$ is Reduced at the Glutathione Binding Site. After GR reduces $AuCl_4^-$, it is inactive toward its cognate substrate, GSSG. The loss of activity occurs over time as GR is incubated with $AuCl_4^-$ in the presence of NADPH, but does not occur in the absence of NADPH. The NADPH-dependent loss of GSSG activity is strong evidence that $AuCl_4^-$ is interacting with the glutathione binding site, and that the reduced gold blocks the catalytic cysteines. Experiments with preformed, 2-nm gold nanoparticles instead of $AuCl_4^-$ produced inactive enzyme rapidly (<1 min) only when NADPH is present. This experiment

(34) Deonarain, M. P.; Scrutton, N. S.; Berry, A.; Perham, R. N. Proceedings: *Biological Sciences* **1990**, *241*, 179−186.

additionally shows that the GR active site is large and flexible enough to bind a spherical 2 nm gold nanoparticle.

That the reduction of $AuCl_4^-$ occurs at the glutathione binding site of GR and that the catalytic cysteine residues participate in this reaction is additionally supported by experiments with GR chemically modified at the catalytic cysteines. Cys42 was alkylated with iodoacetamide in the presence of NADPH, following a literature procedure.[35] This eliminated its ability to reduce GSSG and lowered the $AuCl_4^-$ reduction activity. When NADPH was not included in the alkylation reaction (i.e., Cys42 and Cys47 are disulfide bonded and unreactive toward alkylation), GR activity toward reduction of either GSSG or $AuCl_4^-$ was unaltered by iodoacetamide treatment. These results provide strong evidence that the reduction of $AuCl_4^-$ occurs at the catalytic cysteines.

In an independent experiment, when GR was reacted with H_2O_2 in the presence of NADPH, it lost all activity toward GSSG and $AuCl_4^-$ reduction. Importantly, replacing NADPH by $NADP^+$ (which does not reduce the Cys42-Cys47 active site disulfide to sulfhydryls) in this procedure does not cause a diminution in the activity of GR toward reduction of $AuCl_4^-$. The only reasonable conclusion one can draw from these results is that $AuCl_4^-$ is reduced at the glutathione binding site of GR and that the catalytic cysteines are directly involved in the reduction.

Strikingly, the presence of a gold nanoparticle in the GR active site alters the amount of dimeric enzyme form under denaturing conditions. For GR alone, SDS-PAGE shows <5% of enzyme in the dimeric form under denaturing conditions. Also MALDI-TOF data confirms that GR is predominantly in the monomeric form. SDS-PAGE and MALDI-TOF experiments both show that after GR reduces ~6 atoms of gold, the dimeric form increases in population, and continues to increase with additional $AuCl_4^-$ reduction. The crystal structure of GR shows that the glutathione binding site is located at the interface between the monomers that make the symmetric α_2 dimer. A straightforward interpretation of these results is that the metallic nanoparticle interacts with the side chains from both monomers of the dimer, thereby stabilizing the dimeric structure. Upon the addition of a thiol reagent such as 2-aminoethanethiol or 2-mercoptoethanol, GR returns to its predominantly monomeric form under denaturing conditions since these reagents release the nanoparticle from the GR−AuNP complex.

Reduction of $AuCl_4^-$ Gives Gold Nanoparticles Tightly Bound to GR. NADPH reduction of $AuCl_4^-$, catalyzed by GR, produces metallic gold. TEM images of GR reacted with 280 equiv of $AuCl_4^-$ clearly showed gold nanoparticles of the size expected for 280 atoms of gold (Figure 4). In mass spectroscopy experiments, addition of a given number of equivalents of $AuCl_4^-$ per enzyme resulted in a tightly correlated shift in the mass of GR (Figure 3). This is evidence not only that the gold nanoparticle is attached to GR, but that it remains attached through the harsh condition of the MALDI-TOF sample preparation. Atomic absorption experiments provided additional corroboration that the reduced gold is attached to GR.

The relationship between the number of equivalents of $AuCl_4^-$ added to GR and the peak width in the MALDI-TOF spectra in comparison to unmodified GR suggests a narrow distribution of GR-bound gold nanoparticle sizes. Only a slight broadening of the peak width in the MALDI-TOF spectra is observed. The observed broadening may also be partially due to a distribution of charge states of the GR bound nanoparticle. One explanation for a narrow distribution of nanoparticle size is that the rate of GR catalyzed reduction of $AuCl_4^-$ decreases with increasing nanoparticle size. In this case, the enzymes with fewer atoms of reduced gold will preferentially reduce remaining $AuCl_4^-$ resulting in a rather even distribution nanoparticle size. Spectrophotometric progress curves with $AuCl_4^-$ as the oxidant were nonlinear, unlike with GSSG as the oxidant. They began with a lag phase, sped up, and then slowed again. Although the progress curves have not yet been analyzed in detail, the nonlinearity does indicate that the catalytic activity of GR toward $AuCl_4^-$ reduction varies as the reaction proceeds.

Electron Transfer Between Electrode and Immobilized GR−AuNP Complexes. When unmodified GR is immobilized on TGPE simply by incubating with a buffered enzyme solution, a small flavin peak is observed in CVs at 200 mV/s, demonstrating that direct electron transfer between GR and the TGPE occurs. When a gold nanoparticle is present at the active site of GR, the FAD current significantly increases. For example, oxidation and reduction currents of GR−Au_{250} bound FAD increase ~18 fold compared to FAD bound to unmodified GR.

The reduction and oxidation of FAD involves uptake and release of a proton. The redox potential of FAD bound to GR at pH > 8 is shifted compared to that of FAD alone. Veine et al.[24] identified and explored this shift in FAD potential vs pH. Their work employed alterations in the NADH to NAD^+ ratio in a solution of GR, using spectrophotometric measurement of oxidized and reduced GR-bound flavin.

Here, the redox potential of GR−Au_{50} bound FAD immobilized on TGPE was measured as a function of pH by direct electrochemistry. As pH increased, the potentials were shifted to negative values. At higher pH, the number of protons associated with FAD reduction changed from two to one, with a corresponding change in the slope of the redox potential vs pH plot. This pH dependence is due to active site ionizations that affect flavin reduction. These pH studies show that the current monitored in electrochemical experiments is due to electron transfer to and from GR-bound FAD. It also shows that the flavin binding site of the GR−AuNP complex is not significantly perturbed, since this would result in a change in GR-bound FAD redox potential.

A possible reason why gold nanoparticles increase peak currents as a function of nanoparticle size is that the nanoparticles simply increase the amount of GR immobilized on the TGPE during the 30 min incubation. This hypothesis was tested in EIS experiments, and in direct assays of the amount of GR bound to the TGPE using a spectrophotometric protein assay.

The small (1.5 fold) increase in charge-transfer resistance observed in the EIS experiments when unmodified GR and GR−Au_{250} are compared after a 30 min incubation corresponds to only slightly greater immobilization of GR−Au_{250}, and does not account for the much larger increase in the flavin currents observed in CVs under identical conditions. Additionally, after a 24 h incubation of unmodified GR with the TGPE, a 2-fold increase in charge-transfer resistance is observed as is a 2 fold larger flavin current (data not shown). Yet, even with more

(35) Arscott, L. D.; Thorpe, C.; Williams, C. H., Jr. *Biochemistry* **1981**, *20*, 1513−1520.

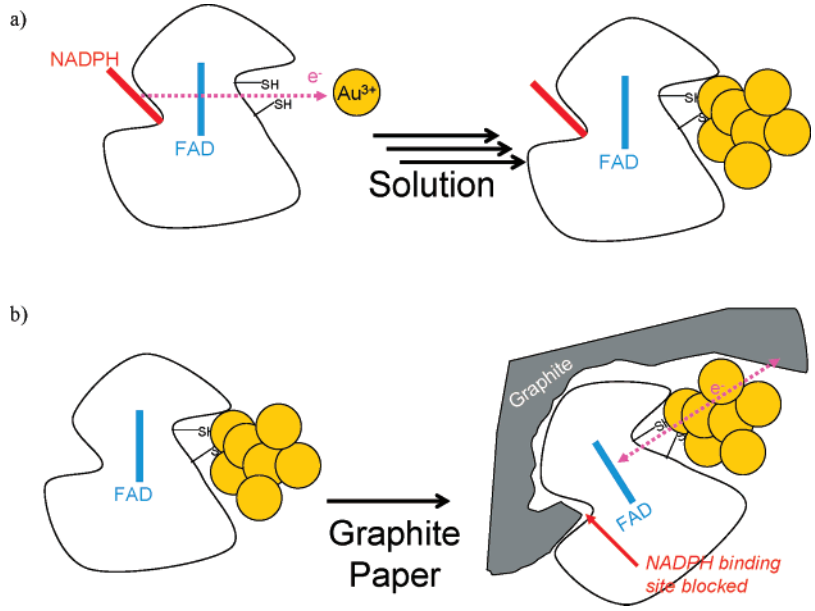

Figure 10. (a) Synthesis of gold nanoparticle at the GR active site. (b) NADPH binding site on GR−AuNP blocked by TGPE.

unmodified GR than GR−Au_{250} immobilized, the flavin current is much larger for GR−Au_{250}. The protein assay experiments, in which the amount of enzyme immobilized was detected after its removal from the electrode with detergent, also failed to find a significant difference in GR−AuNP immobilization as a function of the size of the GR-bound gold nanoparticle (see Supporting Information).

Thus, GR-bound gold nanoparticles facilitate electron transfer between GR-bound FAD and the TGPE. The leveling off of the peak current as a function of AuNP size is co-incident with the transistion of AuNPs from molecular redox behavior to bulk metallic redox behavior.[36] With this in mind, one can conclude that the larger peak currents observed in Figure 6a as AuNP size increases are likely due to more rapid electron transfer between GR-bound FAD and the TGPE due to greater facilitation by the AuNP as it approached bulk metallic behavior.

The peak current in CVs increases linearly as a function of gold nanoparticle size up to ~300 atoms. The CV peak widths, on the other hand, are invariant with gold nanoparticle size and were used to calculate that, independent of nanoparticle size, the redox processes observed correspond to transfer of two electrons. Integration of the current in the oxidation peaks and knowledge of the surface coverage of enzyme allows one to calculate that with GR−Au_{250}, and larger nanoparticles, there are ~2 electrons transferred per enzyme. Therefore, it is concluded that increasing the size of the GR-bound gold nanoparticle allows a greater fraction of the TGPE bound enzyme to be in electrical contact.

Enzyme surface coverage (calculated from cyclic voltammograms under steady-state conditions as the decrease of the real electrode surface area) was estimated to be 9.5×10^{-13} mol cm^{-2}. This corresponds to ~17% electrode surface coverage by GR. The fraction of the bound enzyme that is in electrical contact with the TGPE was estimated from the FAD oxidation peak currents and this knowledge of the surface coverage. For GR, GR−Au_5, GR−Au_{50}, GR−Au_{150}, GR−Au_{250}, and GR−Au_{500}, the calculated values for percent of bound enzyme that is electrically connected are 2, 3, 11, 26, 31, and 31% of the total enzyme coverage, respectively.

Surprisingly, no catalytic current with NADPH was observed with either unmodified GR or GR with any size gold nanoparticle bound. This is a conundrum since: (1) GR−AuNP synthesis in solution using NADPH and $AuCl_4^-$ requires electron transfer from NADPH to GR-bound FAD through the gold nanoparticle to $AuCl_4^-$ in solution, and (2) the CV peaks at the GR-bound FAD potential require electron transfer from reduced flavin through the gold nanoparticle to the TGPE. These results imply that the GR−AuNP NADPH binding site is somehow blocked by the TGPE surface (Figure 10), so that NADPH is incapable of reducing GR-bound FAD.

This hypothesis was tested by replacing NADPH with the much smaller hydride donor BH_4^- as a source of electrons in GR−AuNP CV experiments. BH_4^-, given its small size, is expected to be able to access and reduce FAD without requiring a fully competent NADPH binding site. Previous studies have shown that *E. coli* GR-bound FAD is reduced by BH_4^-.[37] GR−Au_{200} does indeed catalyze electron transfer from BH_4^- to the TGPE: a catalytic current beginning at the FAD potential was observed at a scan rate of 100 mV s^{-1} (Figure 8). GR−Au_{10}, alternatively, does not catalyze electron transfer from BH_4^- to the TGPE. This is consistent with a requirement that the GR-bound AuNP have metallic conductive properties in order to effect catalysis of BH_4^- oxidation.

A smaller and qualitatively different catalytic oxidation current at these lower potentials was also observed for the TGPE modified with 2-nm, premade nanoparticles (Figure 9). This is due to direct oxidation of BH_4^- at the TGPE bound premade gold nanoparticles. At the FAD oxidation potential, the catalytic current for the GR−AuNP modified TGPE electrode is substantially higher. Additionally, the oxidation of BH_4^- on 2 nm

(36) Chen, S.; Ingram, R. S.; Hostetler, M. J.; Pietron, J. J.; Murray, R. W.; Schaaff, T. G.; Khoury, J. T.; Alvarez, M. M.; Whetten, R. L. *Science* **1998**, *280*, 2098−2101.

(37) Scrutton, N. S.; Berry, A.; Deonarain, M. P.; Perham, R. N. *Proc. R. Soc. London, Ser. B* **1990**, *242*, 217−224.

premade AuNP modified TGPE at a scan rate 100 mV s^{-1} shows large catalytic currents only at a potential that is ~300 mV higher than that for GR−Au_{200}. These results show that the catalytic currents observed, at least at the FAD redox potential and possibly at all potentials, with GR−Au_{200} are largely due to electrical connection of the GR-bound FAD by the AuNP to the TGPE.

In summary, two major results have been obtained in the studies presented here. The first is that the flavoenzyme glutathione reductase employs its cognate electron-transfer mechanism to reduce Au^{3+} ions that form a gold nanoparticle tightly bound at the glutathione binding site. The second is that the GR−AuNP complexes show greatly enhanced electron transfer between GR-bound FAD and the TGPE, and catalytically oxidize BH_4^- when the GR-bound nanoparticle is large enough to be electrically conductive. These results suggest novel applications of enzymes as nanoassemblers of composite nanomaterials with controlled properties and catalytic activities.

Acknowledgment. This research was supported by an Office of Naval Research (ONR) award N000140510471.

Supporting Information Available: Experimental details for the EIS and protein assay studies of GR and GR−AuNP immobilized on TGPE, the correlation between number of added $AuCl_4^-$ per GR in solution, and the number of metallic Au atoms found by atomic absorption, and SDS-PAGE of monomeric and dimeric forms of GR and GR−AuNP as a function of 2-aminoethanethiol. This material is available free of charge via the Internet at http://pubs.acs.org.

JA074660G